Brain Imaging and Behavior (2012) 6:584–598
DOI 10.1007/s11682-012-9180-5

ADNI: FRIDAY HARBOR 2011 WORKSHOP SPECIAL ISSUE

Cortical signatures of cognition and their relationship to Alzheimer's disease

Alden L. Gross · Jennifer J. Manly · Judy Pa · Julene K. Johnson · Lovingly Quitania Park · Meghan B. Mitchell · Rebecca J. Melrose · Sharon K. Inouye · Donald G. McLaren · for the Alzheimer's Disease Neuroimaging Initiative

Published online: 21 June 2012

Abstract Recent changes in diagnostic criteria for Alzheimer's disease (AD) state that biomarkers can enhance certainty in a diagnosis of AD. In the present study, we combined cognitive function and brain morphology, a potential imaging biomarker, to predict conversion from mild cognitive impairment to AD. We identified four biomarkers, or cortical signatures of cognition (CSC), from regressions of cortical thickness on neuropsychological factors representing memory, executive function/processing speed, language, and visuospatial function among participants in the Alzheimer's Disease Neuroimaging Initiative (ADNI). Neuropsychological factor scores were created from a previously validated multidimensional factor structure of the neuropsychological battery in ADNI. Mean thickness of each CSC at the baseline study visit was used to evaluate risk of conversion to clinical AD among participants with mild cognitive impairment (MCI) and rate of decline on the Clinical Dementia Rating Scale Sum of Boxes (CDR-SB) score. Of 307 MCI participants, 119 converted to AD. For all domain-

Data used in preparation of this article were obtained from the Alzheimer's Disease Neuroimaging Initiative (ADNI) database (adni.loni.ucla.edu). As such, the investigators within the ADNI contributed to the design and implementation of ADNI and/or provided data but did not participate in analysis or writing of this report. A complete listing of ADNI investigators can be found at: http://adni.loni.ucla.edu/wpcontent/uploads/how_to_apply/ADNI_Acknowledgement_List.pdf

Electronic supplementary material The online version of this article (doi:10.1007/s11682-012-9180-5) contains supplementary material, which is available to authorized users.

A. L. Gross (✉) · S. K. Inouye
Institute for Aging Research, Harvard Medical School, Hebrew SeniorLife, 1200 Centre Street, Rm. 634, Boston, MA, USA
e-mail: aldengross@hsl.harvard.edu

S. K. Inouye
e-mail: sharoninouye@hsl.harvard.edu

A. L. Gross · S. K. Inouye
Division of Gerontology, Beth Israel Deaconess Medical Center, Boston, MA, USA

J. J. Manly
Taub Institute for Research on Alzheimer's Disease and the Aging Brain, Department of Neurology, Columbia University Medical Center, New York, NY, USA
e-mail: jjm71@columbia.edu

J. Pa · J. K. Johnson
Department of Neurology, University of California, San Francisco, CA, USA

J. Pa
e-mail: judy.pa@ucsf.edu

J. K. Johnson
e-mail: Julene.Johnson@ucsf.edu

J. K. Johnson
Institute for Health and Aging; Department of Social and Behavioral Sciences, University of California, San Francisco, CA, USA

L. Q. Park
Department of Neurology, University of California, Davis, CA, USA
e-mail: lovingly.quitania@ucdmc.ucdavis.edu

specific CSC, a one standard deviation thinner cortical thickness was associated with an approximately 50 % higher hazard of conversion and an increase of approximately 0.30 points annually on the CDR-SB. In combined models with a domain-specific CSC and neuropsychological factor score, both CSC and factor scores predicted conversion to AD and increasing clinical severity. The present study indicated that factor scores and CSCs for memory and language both significantly predicted risk of conversion to AD and accelerated deterioration in dementia severity. We conclude that predictive models are best when they utilize both neuropsychological measures and imaging biomarkers.

Keywords MRI · Freesurfer · Cortical thickness · ADNI · Cognition · Brain mapping

Introduction

Alzheimer's disease (AD) is a progressive, devastating, and ultimately fatal neurodegenerative disorder of older age that leads to loss of memory and the ability to function independently (Blennow et al. 2006; Mayeux and Sano 1999). Advances have been made over the past several decades in understanding the pathological cascade of deterioration in AD (Jack et al. 2010). However, the field continues to struggle with how to identify individuals at the highest risk of developing signs and symptoms of clinical AD. The pathological cascade of AD likely begins 20 to 30 years before clinical onset when an individual is still cognitively normal (Weiner et al. 2012). Thus, early detection of AD pathology using biomarkers is of practical and clinical relevance (Clark et al. 2008; Shaw 2008). Correctly distinguishing AD pathology from other neurodegenerative disorders of late life using biomarkers in the preclinical stage of AD would enhance clinical trials for early detection and treatment.

Structural imaging, which facilitates estimation of cortical thickness across the entire cortical surface, is becoming increasingly used in dementia evaluation to assist with differential diagnosis (Hill 2010). Magnetic resonance imaging (MRI) is helpful for excluding other brain conditions that cause cognitive decline, such as brain tumors and hydrocephalus. This shift in clinical practice makes cortical thickness estimation a potentially appealing, feasible biomarker. Structural MRI measures can potentially uncover subtle changes that predict progression to clinical AD (Dickerson et al. 2011). Cortical thickness has been demonstrated to be sensitive to early pathological changes in AD progression. Fennema-Notestine et al. (2009) reported a pattern of greater levels of cortical atrophy from cognitively normal older adults to single-domain MCI patients, multiple-domain MCI patients, and patients with AD. Other studies report similar patterns but have focused on particular brain regions such as the mesial temporal lobe (Karow et al. 2010; McDonald et al. 2009; McEvoy et al. 2009). In a recent study of neuropsychological and MRI characteristics, patients with prodromal AD were identified using new criteria proposed to identify patients early in the disease course. Relative to healthy older adults, patients with prodromal AD presented with greater gray matter atrophy in the medial temporal lobe, which was correlated with lower episodic memory function (Rami et al. 2012). This region is associated with pathological changes early in the course of AD, and the finding underscores the potential utility of establishing an imaging signature of AD.

Previous research has suggested an early link between cortical atrophy in disease-specific brain regions and progression from mild cognitive impairment to AD (Fox et al. 1996, 2001; Schott et al. 2003). The magnitude of cortical thinning in brain regions affected by AD pathology, called a cortical signature of AD, has been shown to predict prodromal AD (Bakkour et al. 2009; Dickerson et al. 2009, 2011). Although research suggests the biology of AD involves a stereotypical pattern of cortical atrophy that begins in medial temporal lobe structures, leading to memory impairment, additional brain regions are affected as the disease progresses, causing deficits in other cognitive functions such as visuospatial function and language. In addition to memory, declines in executive function may take place relatively early in the disease process (Carlson et al. 2008; Johnson et al. 2012), underscoring the importance of multi-domain cognitive assessment to characterize early changes attributable to AD pathology. Thus, assessing the cortical signatures of particular cognitive domains may reveal cortical regions that predict dementia onset and functional progression.

In 2011, the National Institute on Aging Alzheimer's Association workgroup released revised criteria for the diagnosis of AD (McKhann et al. 2011), which called for

M. B. Mitchell · D. G. McLaren
Geriatric Research Education and Clinical Center, Edith Nourse Rogers Memorial Veterans Hospital,
Bedford, MA, USA

M. B. Mitchell
e-mail: Meghan.Mitchell@va.gov

D. G. McLaren
email: mclaren@nmr.mgh.harvard.edu

M. B. Mitchell · D. G. McLaren
Department of Neurology, Massachusetts General Hospital,
Boston, MA, USA

R. J. Melrose
VA Greater Los Angeles Healthcare System; and Dept. of Psychiatry & Biobehavioral Sciences, UCLA,
Los Angeles, CA, USA
e-mail: rjmelrose@ucla.edu

D. G. McLaren
Athinoula A. Martinos Center for Biomedical Imaging,
Department of Radiology, Massachusetts General Hospital,
Charlestown, MA, USA

research on using biomarkers in future diagnostic criteria. McKhann and colleagues concluded that advancements in biomarkers could enhance the pathophysiological specificity of the diagnosis. Amyloid imaging has been suggested as a feasible biomarker, and is currently under FDA review for identifying people with significant amyloid deposition because it may help identify cognitively normal prodromal individuals who may not yet have clinical AD (Sperling et al. 2011). However, evidence of amyloid deposition does not capture everyone at risk, as many older adults with mild cognitive impairment do not have measureable amyloid levels (Villemagne and Rowe 2011). It is also currently unclear whether individuals with mild cognitive impairment without significant amyloid will accumulate significant amyloid and then convert to AD or another dementia.

Previous research using imaging markers have focused either on a priori selected regions (e.g., Fox et al. 2001; Good et al. 2002; Jack et al. 1999; Smith et al. 2007; Thompson et al. 2001), regions with differences between healthy controls and patients with AD (e.g., Davatzikos et al. 2011; Dickerson et al. 2009, 2011), or many regions used in machine learning algorithms with or without feature selection (e.g., Hinrichs et al. 2009, 2011; Misra et al. 2009; Shen et al. 2010). This previous work has established a critical knowledge base and highlights the importance of considering systems of brain regions in the disease process (Ahn et al. 2011; Seeley et al. 2009). Thus, in the present study we aimed to define core brain regions associated with cognitive factors (memory, executive function/processing speed, language, visuospatial function, attention) previously derived from the neuropsychological battery used in ADNI (Park et al. 2012).

The present study investigated whether cortical thinning associated with specific cognitive functions (i.e., cortical signatures of cognition) predicts clinical conversion to AD in older adults with amnestic MCI, and whether the predictive value is independent of a general pattern of cortical thinning that has previously been identified as the cortical signature of AD (Dickerson et al. 2009). Domain-specific factor scores of cognitive function, constructed from a previously established battery of neuropsychological tests (Park et al. 2012), were correlated with regional cortical thickness. It was hypothesized that domain-specific cortical signatures of cognition (CSC), particularly for memory, are associated with time to conversion to AD and worsening function.

Methods

Participants

Data were obtained from the Alzheimer's Disease Neuroimaging Initiative (ADNI) database. ADNI was launched in 2004 by the National Institute on Aging, the National Institute of Biomedical Imaging and Bioengineering, the Food and Drug Administration, private pharmaceutical companies, and non-profit organizations as a $60 million, five-year public-private partnership (Mueller et al. 2005). The primary goal of ADNI was to test whether serial MRI, positron emission tomography (PET), other biological markers, and clinical and neuropsychological assessment can be combined to measure the progression of mild cognitive impairment and early AD. Data, which are continuously updated and freely available to subscribers, were downloaded on March 15, 2011.

Inclusion and diagnostic criteria

ADNI includes participants between 55 and 90 years of age who had a study partner able to provide an independent evaluation of functioning and who spoke either English or Spanish. Participants were primarily recruited from Alzheimer's Disease Research centers. Participants were willing and able to undergo test procedures, including neuroimaging, and agreed to longitudinal follow up. Participants taking certain psychoactive medications were excluded. Healthy control participants had a Mini-Mental State Examination (Folstein et al. 1975) score above 23, clinical dementia rating (CDR) of 0 (Morris 1993), and no depression as measured by the Geriatric Depression Scale (Brink et al. 1982). MCI participants had an MMSE score above 23, CDR of 0.5, and presented with a memory complaint and objective memory impairment measured by the Wechsler Memory Scale Logical Memory Test II (Wechsler 1987). MCI participants had preserved activities of daily living and an absence of dementia. Participants with AD at baseline had an MMSE score between 20 and 26, CDR of 0.5 or 1.0, and met National Institute of Neurological and Communicative Diseases and Stroke/Alzheimer's Disease and Related Disorders Association guidelines (NINCDS/ADRDA) for probable AD (McKhann et al. 1984).

The present study used baseline neuropsychological test performance data and cortical thickness measurements from 119 with MCI who later converted to AD with in 48 months of the baseline visit (MCI-converters) to identify CSC. Baseline and 6, 12, 18, 24, 36, and 48-month follow up data were then used in 307 MCI (of 397) participants to predict conversion to AD and the rate of change in dementia severity. Participants with MCI who later converted to AD were also compared to 169 healthy controls (of 229) to create a cortical signature of AD (Dickerson et al. 2009). Participants were excluded from this study if any of their regional mean cortical thickness measures were greater than 3 standard deviations from their diagnostic group mean after controlling for age, sex, and education. This criterion was chosen to provide an automated method of quality control

rather than manual inspection and editing of the surfaces, which is time-consuming and prone to bias.

Magnetic resonance imaging (MRI)

MRI data were downloaded from the ADNI website. The description of MRI data acquisition of the ADNI study can be found at http://www.adni-info.org/Scientists/MRIProtocols.aspx. Briefly, high-resolution sagittal 3-dimensional T1-weighted Magnetization Prepared RApid Gradient Echo (MP-RAGE) scans using custom designed sequences with voxel sizes of 1.1×1.1×1.2 mm were collected on 1.5 T scanners. MPRAGE sequences were optimized for each scanner to maximize compatibility across scanners. Scanners at each site were calibrated for ADNI with ongoing quality assurance examinations using a specially designed ADNI phantom and human volunteers; these scans were quality-checked by investigators at the Mayo site (Kruggel et al. 2010; Weiner et al. 2012).

Cortical thickness estimation

We applied the FreeSurfer pipeline (version 5.1; Dale et al. 1999; Prabhakaran et al. 2012) to the downloaded MR images to produce cortical thickness measurements for each subject in the ADNI dataset. The T1-weighted MR image was first transformed to the Talairach atlas (Talairach and Tournoux 1988). Next, the main body of white matter was identified by atlas location, intensity, and local neighbors. The variation in intensity across white matter was used to correct bias in the image. The image was then skull stripped, leaving only the brain. The remaining voxels were classified as white matter or non-white matter based on intensity and neighbor constraints. For each hemisphere, an initial surface was created along the edge of white matter and refined to follow the white matter/gray matter intensity gradient. This surface was then pushed outward until the intensity gradient between gray matter and cerebrospinal fluid was reached (the pial surface) (Dale et al. 1999; Fischl and Dale 2000). Next, the sulcal and gyral pattern was aligned to the Freesurfer average surface (Fischl et al. 1999a, b). The surface was resampled into a common reference space, with the same number of nodes, or points, on the surface to analyze the results across participants vertex-by-vertex or regionally. Finally, the thickness values were smoothed with a 10 mm full-width at half maximum Gaussian filter. These methods of determining cortical thickness from MRI scans have been demonstrated to be highly reliable in previous studies of older adults (Dickerson et al. 2008).

Factor scores of cognitive domains

Domain-specific factor scores were created from a previously established factor analysis of the ADNI neuropsychological battery representing memory, executive function/processing speed, visuospatial function, language, and attention (Park et al. 2012). Scores were generated from a confirmatory factor analysis of the following tests administered at the baseline ADNI visit, which allowed the following indicators to have different factor loadings, or weights, on the underlying constructs. Details about administration and scoring of each test are available from the ADNI protocol and elsewhere (Mueller et al. 2005). In consultation with empirical data distributions of each indicator, a consensus panel of neuropsychologists agreed on the factor structure. Memory was represented by the learning (Trial5—Trial1), long delay recall, recognition, and short delay recall calculated from the Auditory Verbal Learning Test (AVLT; Rey 1964) and delayed recall and recognition measures from the ADAS-Cog (Rosen et al. 1984). Visuospatial function was represented by clock-drawing, clock-copy (Goodglass and Kaplan 1983), and ADAS-Cog construction praxis scores. Language was represented by semantic fluency from the Verbal Fluency Test (Morris et al. 1989), spontaneous recall from the Boston Naming Test (Williams et al. 1989), and ADAS-Cog Naming. A factor representing executive function and processing speed was composed of the Trail-Making Test (A and B-A) (Reitan 1958), ADAS-Cog number cancellation, and the digit symbol substitution test (Lezak et al. 2004; Wechsler 1987). Attention was represented by the Digit Span Forward and Backward performance scores (Wechsler 1987). As demonstrated by Park et al. (2012), the factors identified above are invariant across levels of clinical dementia severity.

Clinical Dementia Rating Scale—Sum of Boxes (CDR-SB)

The CDR is a semi-structured interview designed to assess global dementia severity using six categories of cognitive and daily functioning (memory, orientation, judgment and problem solving, community affairs, home and hobbies, and personal care) (Morris 1993). It is useful for staging and tracking decline in AD. Domains in the CDR are rated on an ordinal scale (0=no impairment, 0.5=questionable impairment, 1=mild impairment, 2=moderate impairment, 3=severe impairment), which are summed to create a global estimate of dementia severity (theoretical range=0–18).

Analysis plan

Descriptive statistics were used to characterize the study sample. We used neuropsychological test scores from MCI-converters to identify CSC at the baseline ADNI study visit, which were then used as predictors in survival analyses to predict conversion from MCI to clinical AD and in growth models predicting decline in CDR-SB.

Cortical signatures We identified cortical signatures in the MCI-converter group at baseline and then applied them to

cognitively normal healthy control and MCI groups. For each cognitive domain (memory, executive function/processing speed, language, visuospatial function, attention), multiple regression analyses with covariates for age, sex, and education were performed to evaluate the relationship between cortical thickness and cognitive factor scores across MCI-converter participants. Corresponding cortical thickness regions in all participants with MCI were then used to predict conversion from MCI to AD and functional decline. Five CSCs were identified as the nodes that had a significant ($p<0.005$) relationship between thickness and a factor score (Fig. 1). We excluded the attention CSC from further analyses because it overlapped considerably with other cortical signatures (Table S2). The mean thickness for each CSC was standardized to z-scores in the present study using the mean and standard deviation (e.g. unit variance) in the ADNI healthy control group to ensure that each signature had a comparable variance. The standardized scores were then used to predict conversion from MCI to AD and functional decline.

To compare our CSCs to the previously identified cortical signature of AD (Dickerson et al. 2009), a two-sample *t*-test with covariates for age, sex, and education was used to identify a cortical signature of AD by comparing cortical thickness values in cognitively normal controls versus AD. The cortical signature of AD was created using a threshold at $P<1*10^{-14}$ to make it similar in size to the CSCs. A control region unassociated with any factor scores was created with cortical thickness measures from the calcarine region, which has been used as a control region in previous research (Dickerson et al. 2009).

MCI to AD conversion To accommodate varying times to AD conversion and censoring, we used semi-parametric Cox proportional hazards models to predict conversion to AD within 4 years of follow up using CSC in the MCI sample (Cox 1972). These models provide a relative hazard, which approximates a relative risk, of AD conversion per unit difference in a CSC. As a control, the AD signature and calcarine cortical control regions were included as predictors in a separate model. The timescale used was time from the baseline study visit. Participants stopped contributing time to the analysis when they converted, dropped out of the study, or reached their last study visit without converting. Cumulative probabilities of conversion were plotted using non-parametric Kaplan-Meier curves for each quartile of cortical thickness for each CSC (Kaplan and Meier 1958). Additionally, the following models were estimated: (1) a combined model that included all cortical signatures and the cortical signature of AD; (2) a combined model that included all neuropsychological factor

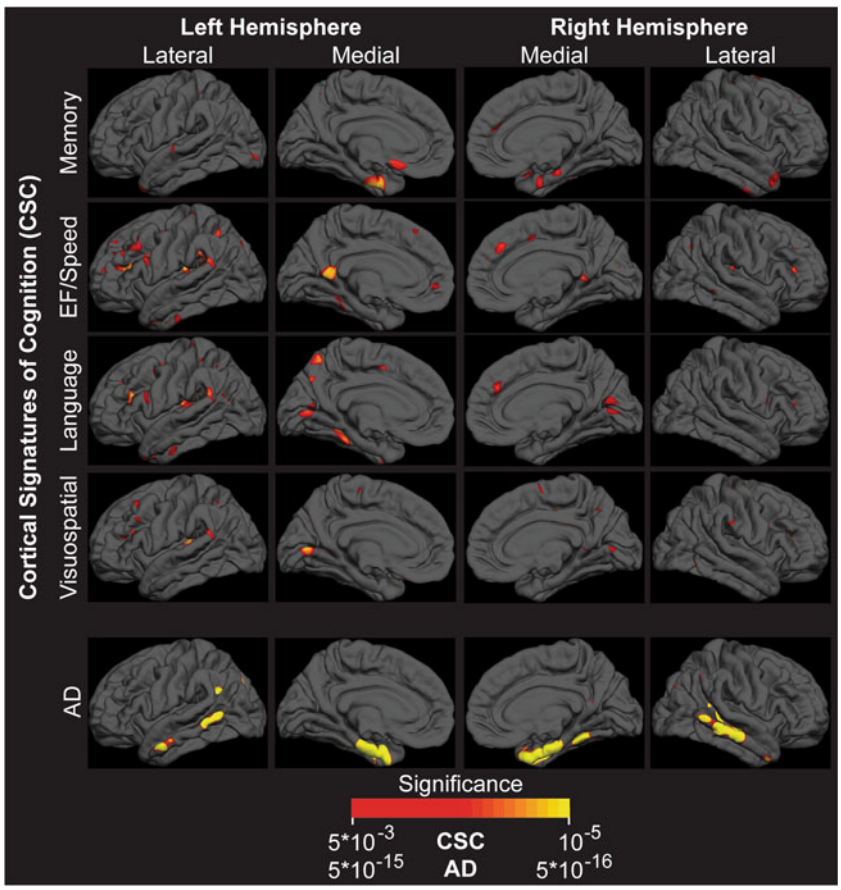

Fig. 1 Graphical representation of domain-specific cortical signatures of cognition (CSC) and the cortical signature of AD. Significant nodes ($P<0.005$) from regressions of cortical thickness and cognitive factor scores are highlighted on the pial surface of the FreeSurfer average brain. To derive the cortical signature of AD, nodes with significant cortical thinning observed between individuals with AD and healthy controls ($P<1*10^{-14}$) are shown on the pial surface of the FreeSurfer average brain. The more stringent threshold for the cortical signature of AD was chosen to create a signature with approximately the same size as the CSC

scores; and (3) CSC and factor score pairs for each cognitive domain. These analyses were conducted using Stata software, version 12 (StataCorp 2011).

All models were adjusted for age, sex, and education. For survival analyses, model fit and the proportional hazards assumption was evaluated using visual displays including Kaplan-Meier plots and graphical displays of Schoenfeld residuals (Hosmer and Lemeshow 1999).

Change in clinical severity Latent growth models were used to model the trajectory of decline in CDR-SB score through the third annual follow up visit (Muthén 1997; Muthén and Curran 1997). Data from the four-year follow up visit were not included for this set of analyses because data collection was still underway at the time this study was conducted. In these models, latent intercept and slope factors represent initial status and annual linear trajectory of CDR-SB score. These latent growth factors were regressed on each CSC in separate models. Coefficients for intercept outcomes represent differences in the baseline CDR-SB score per standard deviation difference in cortical thickness of a CSC. Coefficients for trajectories represent annual paces of change in CDR-SB score per standard deviation difference in cortical thickness of a CSC. Similar to survival analyses predicting conversion, the following models were additionally evaluated: (1) a combined model that included all cortical signatures and the cortical signature of AD; (2) a combined model that included all neuropsychological factor scores; and (3) CSC and factor score pairs for each cognitive domain.

All models were adjusted for sex, age, and education. Model fit for latent growth models was summarized by the root mean square error of approximation (RMSEA; Steiger 1989) and comparative fit index (CFI; Hu and Bentler 1999). An RMSEA less than 0.05 and CFI above 0.95 indicate excellent model fit (Hu and Bentler 1999). These analyses were conducted using Mplus statistical software, version 6.11 (Muthen and Muthen 1998–2010).

Results

Demographics

Descriptive statistics of the sample and neuropsychological measures are in Table 1. The majority of participants were white, male, and college-educated, and the median age was 75 years (range 55, 90). Means and standard deviations of neuropsychological factor scores and component test scores are provided for healthy control, MCI, and AD participants included in the present study whose cortical thickness measures were within 3 standard deviations of their respective group mean. Participants excluded for having cortical thickness measures that exceeded this threshold (healthy control, $n=50$; MCI, $n=90$; AD, $n=46$) did not differ from those in the study on any demographic variables within a diagnostic group after controlling for multiple comparisons. Participants with MCI and AD performed significantly worse on all tests compared to healthy controls. The memory factor score revealed that MCI participants' performance was on average 1.9 standard deviations below that of healthy controls and other neuropsychological factor scores revealed an approximately 1.0 standard deviation difference between healthy control and MCI participants (Table 1).

Cortical Signatures of Cognition (CSC)

CSC for each cognitive domain were defined as all vertices on the cortical surface with a significant correlation between cortical thickness and factor scores ($p<0.005$) and shown on the cortical surface from FreeSurfer in Fig. 1. The anatomical location of the peak of each cluster was determined with the Destriaeux atlas (Destrieux et al. 2010) and listed in Table S1. Each CSC for the MCI group was standardized to its corresponding mean and standard deviation in the healthy control group for use in regressions.

The memory CSC covered 3,176 vertices (Fig. 1; Table S1). The memory CSC overlapped the most with the cortical signature of AD (Table S2). The mean thickness of the memory CSC in cognitively normal participants was 2.85 mm (standard deviation, SD, 0.13 mm). In the MCI group, the mean memory CSC was 2.70 mm (SD=0.19) or 1.11 SD lower than the mean among cognitively normal participants (Table 1).

The executive function/processing speed CSC covered 7,655 vertices (Fig. 1; Table S1). The executive function/processing speed CSC overlapped the most with the language CSC and minimally with the memory CSC, visuospatial CSC, attention CSC, or the cortical signature of AD (Table S2). The executive function/processing speed CSC mean thickness in cognitively normal adults was 2.33 mm (SD=0.11 mm). In the MCI group, the mean executive function/processing speed CSC was 2.24 mm (SD=0.13 mm) or 0.78 SD lower than the mean among cognitively normal participants (Table 1).

The language CSC covered 6,190 vertices (Fig. 1; Table S1). The language CSC overlapped most with the executive function/processing speed CSC and minimally with other signatures (Table S2). The language CSC mean thickness in cognitively normal adults was 2.21 mm (SD=0.10 mm). In the MCI group, the mean language CSC was 2.13 mm (SD=0.12 mm) or 0.79 SD lower than the mean among cognitively normal participants (Table 1).

The visuospatial CSC covered 3,439 vertices (Fig. 1; Table S1). The visuospatial CSC overlapped the most with the executive function/processing speed and language CSC and minimally with other signatures (Table S2). The visuospatial CSC mean thickness in cognitively normal adults

Table 1 Baseline demographic characteristics and cognitive performance: results from ADNI (n=623)

Variable	Healthy control (n=169)	Mild cognitive impairment (n=307)	Alzheimer's disease (n=147)	P-value for group differences
Demographics				
Age, *Median*	75.0	75.0	75.0	0.56
Years of education, *Mean (SD)*	15.9 (2.8)	15.6 (3.1)	14.6 (3.2)	<0.001
Sex, Male, *n (%)*	81 (47.9)	195 (63.5)	82 (55.8)	<0.01
Race, White, *n (%)*	155 (91.7)	287 (93.5)	139 (94.6)	0.69
Mini-Mental State Exam, *Mean (SD)*	29.2 (0.9)	27.1 (1.8)	23.6 (1.9)	<0.001
CDR sum of boxes, *Mean (SD)*	0.0 (0.1)	1.6 (0.9)	4.3 (1.6)	<0.001
Memory				
AVLT Learning (Trial 5—Trial 1), *Mean (SD)*	5.8 (2.4)	3.4 (2.3)	1.8 (1.8)	<0.001
AVLT Long Delay (30 min), *Mean (SD)*	7.6 (3.6)	2.8 (3.4)	0.8 (1.7)	<0.001
AVLT Recognition, *Mean (SD)*	12.9 (2.6)	9.6 (3.6)	7.3 (4.0)	<0.001
AVLT Short Delay, *Mean (SD)*	8.3 (3.3)	3.9 (3.2)	1.7 (1.8)	<0.001
ADAS Delayed Recall, *Mean (SD)*	2.8 (1.7)	6.1 (2.3)	8.6 (1.6)	<0.001
ADAS Recognition, *Mean (SD)*	2.7 (2.4)	4.7 (2.7)	6.6 (2.8)	<0.001
Visuospatial function				
Clock Score, *Mean (SD)*	4.9 (0.4)	4.7 (0.5)	4.4 (0.9)	<0.001
Clock Copy Score, *Mean (SD)*	4.7 (0.6)	4.2 (1.0)	3.5 (1.2)	<0.001
ADAS Construction, *Mean (SD)*	0.4 (0.5)	0.5 (0.6)	0.8 (0.6)	<0.001
Language				
Verbal Fluency Test-Animal total, *Mean (SD)*	20.2 (5.3)	16.3 (4.9)	12.7 (4.6)	<0.001
Verbal Fluency Test-Vegetables, *Mean (SD)*	14.9 (4.0)	10.9 (3.5)	8.2 (3.2)	<0.001
Boston Naming Test, spontaneous recall, *Mean (SD)*	27.3 (2.8)	25.4 (3.6)	23.6 (3.9)	<0.001
ADAS Naming, Any correct, *n (%)*	9 (5.3)	74 (24.1)	56 (38.1)	
Executive function/processing speed				
Trails B-A time, *Mean (SD)*	47.4 (29.3)	72.1 (45.6)	98.1 (57.7)	<0.001
Trails A, *Mean (SD)*	35.4 (12.3)	41.5 (16.6)	58.8 (29.2)	<0.001
ADAS Number Cancellation, *Mean (SD)*	24.9 (5.1)	22.1 (6.0)	18.0 (6.6)	<0.001
Digit Symbol, *Mean (SD)*	45.9 (9.6)	37.7 (10.9)	28.2 (12.4)	<0.001
Attention				
Digit Span Forward, *Mean (SD)*	8.8 (2.0)	8.3 (2.0)	7.5 (1.9)	<0.001
Digit Span Backward, *Mean (SD)*	7.2 (2.0)	6.3 (1.8)	5.3 (1.5)	<0.001
Factor scores (standardized in healthy controls)				
Memory	0.0 (1.0)	−1.1 (1.1)	–	<0.001
Visuospatial function	0.0 (1.0)	−0.4 (0.8)	–	<0.001
Language	0.0 (1.0)	−0.6 (0.8)	–	<0.001
Executive function/processing speed	0.0 (1.0)	−0.5 (0.9)	–	<0.001
Attention	0.0 (1.0)	−0.3 (0.9)	–	<0.001
Cortical signatures (standardized in healthy controls)				
Memory	0.0 (1.0)	−1.1 (1.4)	–	<0.001
Visuospatial function	0.0 (1.0)	−0.7 (1.2)	–	<0.001
Language	0.0 (1.0)	−0.8 (1.2)	–	<0.001
Executive function/processing speed	0.0 (1.0)	−0.8 (1.2)	–	<0.001
Attention	0.0 (1.0)	−0.8 (1.3)	–	<0.001
Control region	0.0 (1.0)	−0.3 (1.2)	–	<0.01
AD pathology	0.0 (1.0)	−1.4 (1.5)	–	<0.001

All neuropsychological domain-specific factor scores and cortical signatures were scaled to have a mean of 0 and standard deviation of 1 in the healthy control group

CDR clinical dementia rating, *M* mean, *SD* standard deviation

was 2.16 mm (SD=0.10 mm). In the MCI group, the mean visuospatial CSC was 2.09 mm (SD=0.12 mm) or 0.66 SD lower than the mean among cognitively normal participants (Table 1).

The attention CSC was the smallest, covering 2,503 vertices (Fig. 1; Table S1). The attention CSC overlapped heavily with the executive function/processing speed, language, and visuospatial CSC and minimally with the memory CSC or the cortical signature of AD (Table S2). Because of the high degree of overlap in the attention CSC with other CSC, we do not report analyses with this CSC. The attention CSC mean thickness in cognitively normal adults was 2.32 (SD=0.10 mm). In the MCI group, the mean attention CSC was 2.24 mm (SD=0.13 mm) or 0.75 standard deviations lower than the mean among cognitively normal participants (Table 1).

Cortical signature of AD

The cortical signature of AD covered 7,912 vertices (Fig. 1, Table S1). Although significant portions of the memory CSC overlapped with the AD signature, most of the cortical signature of AD did not overlap with the memory CSC (Table S2). The mean thickness of the cortical signature of AD in cognitively normal adults was 2.94 mm (SD= 0.12 mm). In the MCI group, the mean was 2.77 mm (SD=0.18 mm) or 1.39 standard deviations lower than the mean among cognitively normal participants (Table 1). As with each CSC, the cortical signature of AD in the MCI group, standardized using the mean and standard deviation in the cognitively normal group, were used in regressions.

Calcarine sulcus control region

The calcarine sulcus region from Destriaeux atlas (Destrieux et al. 2010) had 5,851 vertices. The mean thickness in cognitively normal adults was 1.73 mm (SD=0.10 mm). In the MCI group, the mean was 1.69 mm (SD=0.11 mm), or 0.30 SD lower than the mean among cognitively normal participants (Table 1).

MCI to AD conversion

Among the 307 MCI participants, 119 converted to AD between 0.5 years and 4 years after baseline (median follow up: 2 years). Table 2 provides results of survival analyses predicting conversion to AD among MCI participants. After adjusting for age, sex, and education, MCI participants had between a 45 % and 56 % increased hazard of converting to AD per one standard deviation decrease in baseline domain-specific CSC thickness relative to persons with the mean thickness of cognitively normal adults. Thinning in the language CSC had the largest hazard for conversion. Figure 2 demonstrates that MCI participants in the lowest language CSC quartile, with the thinnest cortices, have a 75 % probability of conversion after 4 years. During the same period, fewer than 30 % of MCI participants with the thickest language CSC quartiles converted (Fig. 2, Language panel). Findings were similar for other CSC, except the control region in which thinning was only weakly associated with conversion over the study period (Fig. 2, Table 2).

Analyses combining each CSC with its cognitive factor score and adjusting for age, sex, and education revealed that all CSC and factor scores were significant independent predictors of conversion (Table 3). The combined hazard of conversion for the memory CSC and memory factor score per 1 SD decrease in both cortical thickness and factor score was 0.42 (0.79*0.54), suggesting a 2.3-fold increased hazard of conversion when both the memory CSC and factor score are considered. This combined hazard is larger than the hazard of conversion for the AD signature (Table 2). Other domain-specific

Table 2 Independent predictors of conversion from MCI to AD in ADNI MCI participants (n=307)

Variable	Hazard ratio	95 % Confidence interval
Cortical signatures		
Memory	0.66*	(0.58, 0.76)
Visuospatial	0.70*	(0.59, 0.84)
Language	0.64*	(0.54, 0.75)
Executive function/processing speed	0.64*	(0.54, 0.75)
Control region	0.81*	(0.69, 0.95)
AD pathology region	0.62*	(0.54, 0.70)
Neuropsychological factor score		
Memory	0.47*	(0.37, 0.58)
Visuospatial	0.64*	(0.53, 0.77)
Language	0.56*	(0.45, 0.70)
Executive function/processing speed	0.58*	(0.47, 0.71)

Results of 10 separate Cox proportional hazards regressions predicting time to conversion to AD through up to 48 months since the baseline visit. All models are adjusted for sex, age, and education

AD Alzheimer's disease

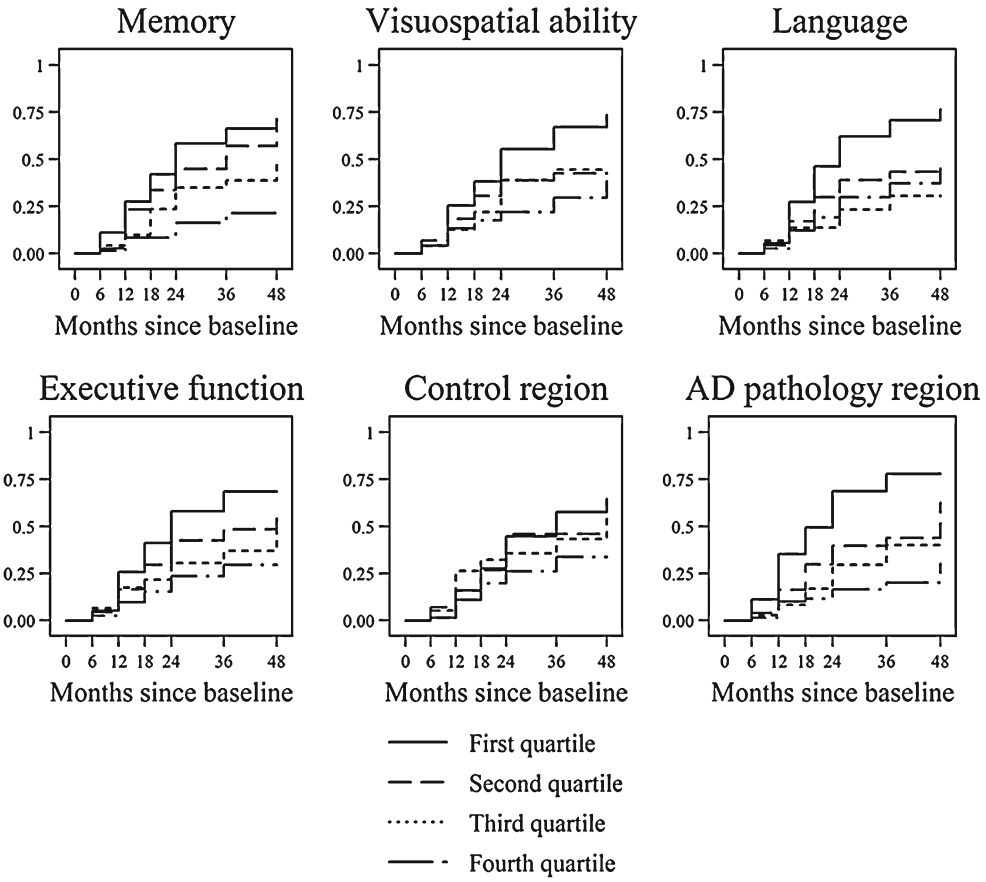

Fig. 2 Cumulative probability of conversion to AD in ADNI MCI participants (n=307). Cumulative probability plots of conversion time to AD for each cortical signature of cognition (CSC), cortical signature of AD, and a control region

combinations similarly increased the hazard of conversion by magnitudes between 1.9 and 2.1, all of which were stronger than the AD signature (Table 2).

In analyses modeling all cortical signatures at once, only the cortical signature of AD emerged as a significant predictor of conversion to AD (Table 4). A model of all factor scores at once revealed that the memory factor score predicted conversion to AD (Table 4). Although other CSC or factor scores were not significantly associated with conversion, they still contributed to the overall hazard of conversion, albeit to a lesser degree.

Change in clinical severity

Results of regressions of levels and trajectories of CDR-SB on domain-specific CSCs are shown in Table 5. Model fit statistics suggested excellent fits to the data (all RMSEA <0.026; all CFI>0.99). Thicker CSC and greater factor

Table 3 Cox proportional hazard survival models of CSC and factor scores in each domain predicting conversion from MCI to AD in ADNI MCI participants (n=307)

Variable	Hazard ratio	95 % Confidence interval
Memory		
Cortical signature of cognition	0.79 *	(0.68, 0.91)
Factor score	0.54 *	(0.42, 0.69)
Visuospatial ability		
Cortical signature of cognition	0.76 *	(0.64, 0.91)
Factor score	0.68 *	(0.57, 0.83)
Language		
Cortical signature of cognition	0.72 *	(0.60, 0.86)
Factor score	0.67 *	(0.53, 0.85)
Executive function/processing speed		
Cortical signature of cognition	0.72 *	(0.60, 0.87)
Factor score	0.68 *	(0.55, 0.85)

Results of 4 separate Cox proportional hazards regressions predicting time to conversion to AD through up to 48 months since the baseline visit. All models are adjusted for sex, age, and education

AD Alzheimer's disease

Table 4 Cox proportional hazard survival models of CSC and factor score predictors of conversion from MCI to AD in ADNI MCI participants (n=307)

Variable	Hazard ratio	95 % Confidence interval
Cortical signatures		
Memory	1.22	(0.89, 1.68)
Visuospatial	1.01	(0.72, 1.41)
Language	0.79	(0.52, 1.22)
Executive function/processing speed	0.91	(0.62, 1.32)
Control region	1.02	(0.84, 1.24)
AD pathology region	0.55 *	(0.40, 0.76)
Neuropsychological factor score		
Memory	0.48 *	(0.37, 0.62)
Visuospatial	0.85	(0.62, 1.17)
Language	1.28	(0.86, 1.91)
Executive function/processing speed	0.76	(0.54, 1.06)

Results of 2 Cox proportional hazards regressions predicting time to conversion to AD through up to 48 months since the baseline visit. The first model included all cortical signatures together. The second model included all neuropsychological factor scores together. Models are adjusted for sex, age, and education

AD Alzheimer's disease

scores predicted lower baseline CDR-SB, with the exception of the control CSC and the visuospatial CSC and factor score. All CSC and factor scores predicted annual increases in CDR-SB as cortical thickness declines and cognitive ability declines, respectively. The memory, language, and AD cortical regions were the strongest predictors of level and change in CDR-SB. For example, for the memory CSC, a 1 SD lower thickness at baseline was associated with a 0.30 unit increase in CDR-SB annually. As expected, the control region had the weakest relationship among the thickness measures.

Results from regressions of levels and trajectories of CDR-SB on domain-specific CSC and its accompanying neuropsychological factor score are summarized in Table 6. As with previous analyses, thinning in the memory CSC areas was significantly associated with steeper decline in CDR-SB after adjusting for the memory neuropsychological factor score. The same was true of other domain-specific CSC, but strongest for memory, language, and executive function/processing speed. Although neuropsychological factor scores were stronger predictors of level and change in CDR-SB than corresponding CSC, CSCs were still significant independent predictors of change in CDR-SB.

When all CSC and the cortical signature of AD were combined in a single growth model to predict trajectory of CDR-SB, greater thickness in every CSC was associated with less baseline impairment and less worsening in CDR-SB over time (Table 7). This was also true when all neuropsychological factor scores were entered into a model together (Table 7).

Discussion

The present study investigated the ability of cortical thickness from CSC, empirically defined by their correlation with domain-specific cognitive factor scores, to predict clinical conversion to AD and accelerated worsening of clinical severity. Cortical thinning in each CSC was associated with faster progression to AD and with faster rates of decline in CDR-SB score. The analyses converge on three main findings. First, domain-specific cortical signatures of cognition can be estimated which are largely independent of the cortical signature of AD. Second, these cortical thickness measurements and cognitive performance account for unique variance in conversion to AD and accelerated worsening of clinical severity (Tables 3 and 6). Third, latent factors representing performance on neuropsychological measures of memory, executive function, and language and their corresponding CSC are the best predictors of conversion to AD and clinically relevant decline in nearly all models.

These results may provide clinicians with the ability to use the ADNI neuropsychological battery in conjunction with a structural MRI scan to provide a more accurate estimate of the risk of conversion to AD. Importantly, in current clinical practice an MRI, which can be conducted in minutes, is almost universally performed in dementia evaluations while neuropsychological testing, which can take an hour or more, is less common. As seen in the results, a 1 SD loss in thickness in the memory CSC and 1 SD decrease in memory function more than doubles the risk of developing clinical AD. Knowledge of AD risk is important for both the treatment of patients and for identifying potential candidates for novel therapeutic interventions.

The present study utilized a large, well-characterized sample of participants to empirically define cortical signatures of cognition. Although the focus of this paper was not about the detailed significance or implications of any particular region or domain, we briefly discuss the CSC and cortical signature of AD in relation to previous research. We leveraged advantages of rigorously constructed factor scores from a confirmatory factor analysis (Park et al. 2012) to identify structure-function relationships. This approach is in

Table 5 Results from regressions of trajectories of CDR sum of boxes on domain-specific cortical regions and neuropsychological factor scores from latent growth models in ADNI MCI participants (n=307)

Variable	Estimate	95 % Confidence interval
Cortical signature of cognition		
Memory		
Intercept	−0.13 *	(−0.21, −0.05)
Trajectory	−0.30 *	(−0.37, −0.22)
Visuospatial		
Intercept	−0.08	(−0.18, 0.01)
Trajectory	−0.24 *	(−0.35, −0.14)
Language		
Intercept	−0.13 *	(−0.21, −0.04)
Trajectory	−0.29 *	(−0.39, −0.19)
Executive function/processing speed		
Intercept	−0.12 *	(−0.21, −0.03)
Trajectory	−0.29 *	(−0.39, −0.19)
Control region		
Intercept	−0.03	(−0.12, 0.06)
Trajectory	−0.12 *	(−0.23, −0.02)
AD pathology region		
Intercept	−0.13 *	(−0.20, −0.06)
Trajectory	−0.30 *	(−0.37, −0.23)
Neuropsychological factor score		
Memory		
Intercept	−0.19 *	(−0.29, −0.09)
Trajectory	−0.42 *	(−0.50, −0.34)
Visuospatial		
Intercept	−0.08	(−0.18, 0.02)
Trajectory	−0.39 *	(−0.50, −0.27)
Language		
Intercept	−0.17 *	(−0.29, −0.05)
Trajectory	−0.44 *	(−0.55, −0.34)
Executive function/processing speed		
Intercept	−0.20 *	(−0.31, −0.10)
Trajectory	−0.40 *	(−0.51, −0.29)

Results of 10 separate latent growth models of CDR-SB through 36 months. Coefficients for intercept outcomes represent differences in CDR sum of box units per unit change in cortical thickness, which is on a z-score metric (mean=0, sd=1). Coefficients for slope outcomes represent annual change in CDR sum of box score per unit difference in cortical thickness measure. Models are adjusted for sex, age, and education

AD Alzheimer's disease

Table 6 Results from regressions of trajectories of CDR sum of boxes on domain-specific cortical regions from latent growth models in ADNI MCI participants (n=307)

Variable	Estimate	95 % Confidence interval
Model 1. Memory		
Cortical signature of cognition		
Intercept	−0.08	(−0.17, 0.01)
Trajectory	−0.18 *	(−0.25, −0.11)
Factor score		
Intercept	−0.14 *	(−0.25, −0.03)
Trajectory	−0.31 *	(−0.39, −0.23)
Model 2. Visuospatial ability		
Cortical signature of cognition		
Intercept	−0.07	(−0.17, 0.03)
Trajectory	−0.15 *	(−0.25, −0.06)
Factor score		
Intercept	−0.05	(−0.15, 0.05)
Trajectory	−0.33 *	(−0.43, −0.22)
Model 3. Language		
Cortical signature of cognition		
Intercept	−0.09	(−0.18, 0.01)
Trajectory	−0.18 *	(−0.28, −0.08)
Factor score		
Intercept	−0.12	(−0.25, 0.01)
Trajectory	−0.34 *	(−0.45, −0.24)
Model 4. Executive function/processing speed		
Cortical signature of cognition		
Intercept	−0.06	(−0.15, 0.04)
Trajectory	−0.18 *	(−0.28, −0.09)
Factor score		
Intercept	−0.17 *	(−0.29, −0.06)
Trajectory	−0.30 *	(−0.41, −0.19)

Results of 5 separate latent growth models of CDR-SB score through 36 months. Coefficients for intercept outcomes represent differences in CDR sum of box units per unit change in cortical thickness, which is on a z-score metric (mean=0, sd=1). Coefficients for slope outcomes represent annual change in CDR sum of boxes score per unit difference in cortical thickness measure. Models are adjusted for sex, age, and education

contrast to testing the relationship of the many variables in the ADNI neuropsychological battery; however, since the goal was to identify regions associated with domains of cognition for use in subsequent analysis, we were less interested in differences within each domain (e.g. encoding versus retrieval) (Walhovd et al. 2010; Wolk and Dickerson 2011).

We can use results from other imaging studies to confirm using examples below that the cortical signatures are measuring each domain accurately (e.g., content validity). For example, the memory CSC is dominated by areas of the mesial temporal lobe that have been shown to be related to memory both in function and structure (Buckner 2004; Buckner et al. 2005; Burggren et al. 2011; Dickerson et al. 2008; Fjell et al. 2008; Johnson et al. 2006). The executive function/processing speed, language, and visuospatial CSC all had significant overlap, but also encompassed unique brain areas. Importantly, our findings emphasize that executive function is not synonymous with frontal lobe

Table 7 Results from regressions of trajectories of CDR sum of boxes on domain-specific cortical regions and neuropsychological factor scores from two latent growth models in ADNI MCI participants (n=307)

Variable	Estimate	95 % Confidence interval
Cortical signature of cognition		
Memory		
Intercept	−0.13 *	(−0.21, −0.05)
Trajectory	−0.30 *	(−0.37, −0.22)
Visuospatial		
Intercept	−0.08	(−0.18, 0.01)
Trajectory	−0.24 *	(−0.35, −0.14)
Language		
Intercept	−0.13 *	(−0.21, −0.04)
Trajectory	−0.29 *	(−0.39, −0.19)
Executive function		
Intercept	−0.12 *	(−0.21, −0.03)
Trajectory	−0.29 *	(−0.39, −0.19)
Control region		
Intercept	−0.03	(−0.12, 0.06)
Trajectory	−0.12	(−0.23, −0.00)
AD pathology region		
Intercept	−0.13 *	(−0.20, −0.06)
Trajectory	−0.30 *	(−0.37, −0.23)
Neuropsychological factor score		
Memory		
Intercept	−0.19 *	(−0.29, −0.09)
Trajectory	−0.42 *	(−0.50, −0.34)
Visuospatial		
Intercept	−0.08	(−0.18, 0.02)
Trajectory	−0.39 *	(−0.50, −0.27)
Language		
Intercept	−0.17 *	(−0.29, −0.05)
Trajectory	−0.44 *	(−0.55, −0.34)
Executive function		
Intercept	−0.20 *	(−0.31, −0.10)
Trajectory	−0.40 *	(−0.51, −0.29)

Results of 2 separate latent growth models of CDR-SB score through 36 months. The first model included all cortical signatures together. The second model included all neuropsychological factor scores together. Coefficients for intercept outcomes represent differences in CDR sum of box units per unit change in cortical thickness, which is on a z-score metric (mean=0, sd=1). Coefficients for slope outcomes represent annual change in CDR sum of box score per unit difference in cortical thickness measure. Models are adjusted for sex, age, and education

AD Alzheimer's disease

functioning and suggests that successful task performance also relies on non-frontal brain regions responsible for other fundamental skills. The language CSC corresponds to regions shown to correlate with the Boston Naming Test and the Controlled Oral Word Association Test (COWAT), both measures of language ability (Ahn et al. 2011). The attention CSC had the fewest vertices, a finding that could be due to acute demands of the tasks. The cortical signature of AD we used is consistent with regions that have previously been shown to be atrophic in AD (Buckner et al. 2005; Dickerson et al. 2009, 2011; Fjell et al. 2009). At lower thresholds, most of the brain is atrophic in large AD samples. We chose a high threshold to constrain the signature to be the approximate size of each CSC, but note that alternative thresholds could have been chosen.

Survival plots suggest that there are at least 2 distinct patterns of cortical atrophy in Alzheimer's disease (Fig. 2). Specifically, the middle quartiles of the memory CSC and AD pathology show similar survival curves. In contrast, the visuospatial, executive function/processing speed, and language CSC revealed that the top two quartiles were similar and the bottom two quartiles were similar. These groupings are not surprising given the overlap between CSCs. However, the finding is also consistent with the notion of multiple etiologies of AD (Buckner 2004). Future studies should probe covariance patterns in longitudinal change in cortical thickness to better capture potentially separable processes. It is likely that a combination of behavioral and structural change metrics will be ideal for identifying those at highest risk of conversion to AD and accelerated worsening in clinical severity.

Our results can be contextualized in a hypothetical model of biomarker and cognitive change in pathological AD proposed by Jack and colleagues (Jack et al. 2010). The Jack model proposes that AD pathology begins with abnormal buildup of amyloid beta, which subsequently results in irregular processing of tau protein, leading to neurofibrillary tangles and cellular apoptosis, impaired function in brain systems, cortical thinning in certain brain regions, and eventually cognitive decline and functional disability characteristic of clinical AD. Although the timing and relative order of biomarkers that measure these signs and symptoms is an active area of research, their importance in AD is not disputed. The present results suggest that amount of atrophy predict rate of functional decline, and thus takes place beforehand. This inference is drawn from the finding that, after controlling for neuropsychological factor scores as indices of behavior that were used to define the CSC, the CSC still predicted conversion and significantly increased CDR-SB trajectories. Additionally, the memory CSC and neuropsychological score together better predicted conversion from MCI to AD than the cortical signature of AD alone. Although it is not known how amyloid (either measured by PET or CSF samples) would affect the predictive value of the CSC in the present study, PET scans and lumbar punctures are not performed as routinely as MRI at this time. Thus, utilizing a more widely-applied technique to inform the risk of conversion may be preferable.

Although the aim of this work was to investigate conversion from MCI to AD, it is also necessary to predict conversion from cognitively normal to MCI and to AD. At present, this involves identifying individuals with preclinical AD (Sperling et al. 2011), usually with a PET scan for amyloid. However, our study suggests that cognitive function, in combination with cognition-defined signatures of structural or functional MRI, could provide sensitive measures to identify individuals with an increased risk of developing AD that may complement PET imaging. Future research using CSCs is needed to investigate which CSCs best predict conversion among healthy controls to MCI and AD.

This study probed the relationship of behavior and morphometry in predicting conversion to MCI and accelerated worsening in dementia severity. Importantly, we chose to define our morphometry metrics from structure-function relationships based on a validated factor analysis of the ADNI neuropsychological battery (Park et al. 2012), rather than pathological differences. In defining morphometry metrics based on behavior, we were able to target several aspects of the pathological AD disease process. Although memory, executive function, and language provided the dominant effects, thickness in other regions can be used to compute a cumulative odds ratio across CSCs or factor scores.

Several caveats merit attention. First, the ADNI sample is more highly educated than the US population and represents a self-selected sample of volunteers who present to AD research centers. Thus, findings should be replicated in other more educationally and culturally diverse samples. Second, factor scores for particular cognitive domains are, by design, a generalization of performance on cognitive tasks designed to measure very specific aspects of cognitive function. CSC derived from these scores are a further abstraction, which may obscure specific forms of neuropsychological impairment that might predict AD early in its course (Wolk and Dickerson 2011). However, clinical AD defined in ADNI, as predicted in our survival models, is a disease of global impairment. A third caveat is that successful performance in any domain of cognition is not independent of other cognitive domains, and likely entails contributions from several neural networks (Wolk and Dickerson 2011). The present study's CSCs were based on empirically defined brain regions correlated with neuropsychological performance, not neural networks. Thus, domain-specific CSCs in this study are also correlated with each other (Table S3), which has implications for statistical models where all the CSCs are considered at the same time. Finally, the present study did not investigate cortical volumes that were empirically associated with cognitive function. Volumetric analyses, whether using Freesurfer volumes or voxel-based morphometry to identify voxels that are correlated with neuropsychological factors scores, should be explored in future studies.

Conclusion

The ability to accurately identify risk for developing clinical AD while an individual has normal cognition or MCI will enhance selection of participants for treatment trials and enable clinicians to decide on optimal management at an earlier stage. Establishing CSCs is a promising approach that integrates structural imaging with the gold standard of clinical disease stage, neuropsychological measures, and thus enables researchers to track change in multiple modalities over time. The present study indicated that factor scores and CSCs for memory and language both significantly predicted risk of conversion to AD and accelerated deterioration in dementia severity. We conclude that predictive models are best when they utilize both neuropsychological measures and imaging biomarkers.

Acknowledgements We gratefully acknowledge a conference grant from the National Institute on Aging (R13AG030995, PI: Mungas) that facilitated data analysis for this project. Dr. Gross was supported by an NIH Translational Research in Aging fellowship (T32AG023480-07, PI: Lipsitz) and the NIA (P01AG031720, PI: Inouye). Dr. McLaren was supported by NIA grant RO1 AG036694 (PI: Sperling) and K23 AG027171 (PI: Atri). Dr. Bruce Rosen (MGH-Harvard-MIT Martinos Center for Biomedical Imaging) provided guidance, space, and resources for this research. Dr. Johnson was supported by the NIA (R01 AG022538, PI: Johnson). Dr. Melrose was supported by a VA Career Development Award & UCLA Semel Scholar Award. Dr. Pa was supported by the NIA Career Development Award (K01 AG034175, PI: Pa). Dr. Park was supported by a grant from the National Institute of Aging (R01 AG031252 PI: Farias). Dr. Inouye holds the Milton and Shirley F. Levy Family Chair in Alzheimer's Disease.

Data collection and sharing for this project was funded by the Alzheimer's Disease Neuroimaging Initiative (ADNI) (National Institutes of Health Grant U01 AG024904). ADNI is funded by the National Institute on Aging, the National Institute of Biomedical Imaging and Bioengineering, and through generous contributions from the following: Abbott; Alzheimer's Association; Alzheimer's Drug Discovery Foundation; Amorfix Life Sciences Ltd.; AstraZeneca; Bayer HealthCare; BioClinica, Inc.; Biogen Idec Inc.; Bristol-Myers Squibb Company; Eisai Inc.; Elan Pharmaceuticals Inc.; Eli Lilly and Company; F. Hoffmann-La Roche Ltd and its affiliated company Genentech, Inc.; GE Healthcare; Innogenetics, N.V.; Janssen Alzheimer Immunotherapy Research & Development, LLC.; Johnson & Johnson Pharmaceutical Research & Development LLC.; Medpace, Inc.; Merck & Co., Inc.; Meso Scale Diagnostics, LLC.; Novartis Pharmaceuticals Corporation; Pfizer Inc.; Servier; Synarc Inc.; and Takeda Pharmaceutical Company. The Canadian Institutes of Health Research is providing funds to support ADNI clinical sites in Canada. Private sector contributions are facilitated by the Foundation for the National Institutes of Health (www.fnih.org). The grantee organization is the Northern California Institute for Research and Education, and the study is coordinated by the Alzheimer's Disease Cooperative Study at the University of California, San Diego. ADNI data are disseminated by the Laboratory for Neuro Imaging at the University of California, Los Angeles. This research was also supported by NIH grants P30 AG010129, K01 AG030514, and the Dana Foundation.

The contents do not represent the views of the Dept. of Veterans Affairs, the United States Government, or any other funding entities.

References

Ahn, H. J., Seo, S. W., Chin, J., Suh, M. K., Lee, B. H., …, Na, D. L. (2011). The cortical neuroanatomy of neuropsychological deficits in mild cognitive impairment and Alzheimer's disease: a surface-based morphometric analysis. *Neuropsychologia*, *49*(14), 3931–3945.

Bakkour, A., Morris, J. C., & Dickerson, B. C. (2009). The cortical signature of prodromal AD: regional thinning predicts mild AD dementia. *Neurology, 72*(12), 1048–1055.

Blennow, K., de Leon, M. J., & Zetterberg, H. (2006). Alzheimer's disease. *Lancet, 368*, 387–403.

Brink, T. L., Yesavage, J. A., Lum, O., Heersema, P., Adey, M. B., & Rose, T. L. (1982). Screening tests for geriatric depression. *Clinical Gerontologist, 1*, 37–44.

Buckner, R. L. (2004). Memory and executive function in aging and AD: multiple factors that cause decline and reserve factors that compensate. *Neuron, 44*, 195–208.

Buckner, R. L., Snyder, A. Z., Shannon, B. J., LaRossa, G., Sachs, R., …, Mintun, M. A. (2005). Molecular, structural, and functional characterization of Alzheimer's disease: evidence for a relationship between default activity, amyloid, and memory. *Journal of Neuroscience*, *25*(34), 7709–7717.

Burggren, A. C., Renner, B., Jones, M., Donix, M., Suthana, N. A., …, Bookheimer, S. Y. (2011). Thickness in entorhinal and subicular cortex predicts episodic memory decline in mild cognitive impairment. *International Journal of Alzheimer's Disease*, 2011, 956053.

Carlson, M. C., Xue, Q., Zhou, J., & Fried, L. P. (2008). Executive decline and dysfunction precedes declines in memory: the women's health and aging study II. *Journal of Gerontology: Series A: Biological, Social, and Medical Sciences, 64A*, 110–117.

Clark, C. M., Davatzikos, C., Borthakur, A., Newberg, A., Leight, S., Lee, V. M., et al. (2008). Biomarkers for early detection of Alzheimer pathology. *Neurosignals, 16*, 11–18.

Cox, D. R. (1972). Regression models and life-Tables (with discussion). *Journal of the Royal Statistical Society, Series B, 34*, 187–220.

Dale, A. M., Fischl, B., & Sereno, M. I. (1999). Cortical surface-based analysis. I. Segmentation and surface reconstruction. *Neuroimage, 9*, 179–194.

Davatzikos, C., Bhatt, P., Shaw, L. M., Batmanghelich, K. N., & Trojanowski, J. Q. (2011). Prediction of MCI to AD conversion, via MRI, CSF biomarkers, and pattern classification. *Neurobiology* of *Aging*, *32*(12), 2322 e2319–2327.

Destrieux, C., Fischl, B., Dale, A., & Halgren, E. (2010). Automatic parcellation of human cortical gyri and sulci using standard anatomical nomenclature. *NeuroImage, 53*(1), 1–15.

Dickerson, B. C., Fenstermacher, E., Salat, D. H., Wolk, D. A., Maguire, R. P., …, Fischl, B. (2008). Detection of cortical thickness correlates of cognitive performance: reliability across MRI scan sessions, scanners, and field strengths. *Neuroimage*, *39*, 10–18.

Dickerson, B. C., Bakkour, A., Salat, D. H., Feczko, E., Pacheco, J., …, Buckner, R. L. 2009. The cortical signature of Alzheimer's disease: regionally specific cortical thinning relates to symptom severity in very mild to mild AD dementia and is detecTable in asymptomatic amyloid-positive individuals. *Cerebral Cortex*, *19* (3), 497–510 (Mar).

Dickerson, B. C., Stoub, T. R., Shah, R. C., Sperling, R. A., Killiany, R. J., …, Detoledo-Morrell, L. (2011). Alzheimer-signature MRI biomarker predicts AD dementia in cognitively normal adults. *Neurology*, *76*(16), 1395–1402.

Fennema-Notestine, C., Hagler, D. J., Jr., McEvoy, L. K., Fleisher, A. S., Wu, E. H., Karow, D. S., et al. (2009). Structural MRI biomarkers for preclinical and mild Alzheimer's disease. *Human Brain Mapping, 30*, 3238–3253.

Fischl, B., & Dale, A. M. (2000). Measuring the thickness of the human cerebral cortex from magnetic resonance images. *Proceedings of the National Academy of Sciences of the United States of America, 97*(20), 11050–11055.

Fischl, B., Sereno, M. I., & Dale, A. M. (1999a). Cortical surface-based analysis. II: inflation, flattening, and a surface-based coordinate system. *NeuroImage, 9*(2), 195–207.

Fischl, B., Sereno, M. I., Tootell, R. B., & Dale, A. M. (1999b). High-resolution intersubject averaging and a coordinate system for the cortical surface. *Human Brain Mapping, 8*(4), 272–284.

Fjell, A. M., Amlien, I. K., Westlye, L. T., & Walhovd, K. B. (2009). Mini-mental state examination is sensitive to brain atrophy in Alzheimer's disease. *Dementia and Geriatric Cognitive Disorders, 28*(3), 252–258.

Fjell, A. M., Walhovd, K. B. Amlien, I., Bjørnerud, A., Reinvang, I., …, Fladby, T. (2008). Morphometric changes in the episodic memory network and tau pathologic features correlate with memory performance in patients with mild cognitive impairment. *American Journal of Neuroradiology*, *29*(6), 1183–1189.

Folstein, M. F., Folstein, S. E., & McHugh, P. R. (1975). Mini-mental state A practical method for grading the mental state of patients for the clinician. *Journal of Psychiatric Research, 12*, 189–198.

Fox, N. C., Crum, W. R., Scahill, R. I., Stevens, J. M., Janssen, J. C., & Rossor, M. N. (2001). Imaging of onset and progression of Alzheimer's disease with voxel-compression mapping of serial magnetic resonance images. *Lancet, 358*, 201–205.

Fox, N. C., Warrington, E. K., Freeborough, P. A., Hartikainen, P., Kennedy, A. M., …, Rossor, M. N. (1996). Presymptomatic hippocampal atrophy in Alzheimer's disease: a longitudinal MRI study. *Brain*, *119*, 2001–2007.

Good, C. D., Scahill, R. I., Fox, N. C., Ashburner, J., Friston, K. J., …, Frackowiak, R. S. (2002). Automatic differentiation of anatomical patterns in the human brain: validation with studies of degenerative dementias. *Neuroimage*, *17*, 29–46.

Goodglass, H., & Kaplan, E. (1983). *The assessment of aphasia and related disorders*. Philadelphia: Lea & Febiger.

Hill, D. (2010). Neuroimaging to assess safety and efficacy of AD therapies. *Expert Opinion on Investigative Drugs, 19*, 23–26.

Hinrichs, C., Singh, V., Xu, G., & Johnson, S. (2009). MKL for robust Multi-modality AD Classification. *Medical Image Computing and Computer Assisted Intervention, 5762*, 786–794.

Hinrichs, C., Singh, V., Xu, G., Johnson, S. C., & Initiative, Alzheimers Disease Neuroimaging. (2011). Predictive markers for AD in a multi-modality framework: an analysis of MCI progression in the ADNI population. *NeuroImage, 55*(2), 574–589.

Hosmer, D. W., & Lemeshow, S. (1999). *Applied survival analysis: Regression modeling of time to event data*. New York: Wiley.

Hu, L., & Bentler, P. M. (1999). Cutoff criteria for fit indices in covariance structure analysis: conventional versus new alternatives. *Structural Equation Modeling, 6*, 1–55.

Jack, C. R. Jr., Knopman, D. S., Jagust, W. J., Shaw, L. M., Aisen, P. S., …, Trojanowski, J. Q. (2010). Hypothetical model of dynamic biomarkers of the Alzheimer's pathological cascade. *Lancet Neurology*, *9*, 119–128.

Jack, C. R. Jr., Petersen, R. C., Xu, Y. C., O'Brien, P. C., Smith, G. E., …, Kokmen, E. (1999). Prediction of AD with MRI-based hippocampal volume in mild cognitive impairment. *Neurology*, *52* (7), 1397–1403.

Johnson, J. K., Gross, A. L., Pa, J., McLaren, D. G., Park, L. Q., & Manly, J. J., for the Alzheimer's Disease Neuroimaging Initiative (2012). Longitudinal change in neuropsychological performance using

latent growth models: A study of mild cognitive impairment. *Brain Imaging and Behavior*.

Johnson, S. C., Schmitz, T. W., Moritz, C. H., Meyerand, M. E., Rowley, H. A., …, Alexander, G. E. (2006). Activation of brain regions vulnerable to Alzheimer's disease: the effect of mild cognitive impairment. *Neurobiology* of *Aging*, *27*(11), 1604–1612.

Kaplan, E. L., & Meier, P. (1958). Nonparametric estimation from incomplete observations. *Journal of the American Statistical Association, 53*, 457–481.

Karow, D. S., McEvoy, L. K., Fennema-Notestine, C., Hagler, D. J., Jr., Jennings, R. G., Brewer, J. B., et al. (2010). Relative capability of MR imaging and FDG PET to depict changes associated with prodromal and early Alzheimer disease. *Radiology, 256*, 932–942.

Kruggel, F., Turner, J., & Muftuler, L. T. (2010). Impact of scanner hardware and imaging protocol on image quality and compartment volume precision in the ADNI cohort. *NeuroImage, 49*, 2123–2133.

Lezak, M. D., Howieson, D. B., & Loring, D. W. (2004). *Neuropsychological assessment* (p. 472). New York: Oxford University Press.

Mayeux, R., & Sano, M. (1999). Treatment of Alzheimer's disease. *The New England Journal of Medicine, 341*, 1670–1679.

McDonald, C. R., McEvoy, L. K., Gharapetian, L., Fennema-Notestine, C., Hagler, D. J., Jr., Holland, D., et al. (2009). Regional rates of neocortical atrophy from normal aging to early Alzheimer disease. *Neurology, 73*, 457–465.

McEvoy, L. K., Fennema-Notestine, C., Roddey, J. C., Hagler, D. J., Jr., Holland, D., Karow, D. S., et al. (2009). Alzheimer disease: quantitative structural neuroimaging for detection and prediction of clinical and structural changes in mild cognitive impairment. *Radiology, 251*, 195–205.

McKhann, G., Drachman, D., Folstein, M., Katzman, R., Price, D., & Stadlan, E. M. (1984). Clinical diagnosis of Alzheimer's disease: report of the NINCDS-ADRDA group under the auspices of Department of HHS Task Force on Alzheimer's disease. *Neurology, 34*, 939–944.

McKhann, G. M., Knopman, D. S., Chertkow, H., Hyman, B. T., Jack, C. R. Jr., …, Phelps, C. H. (2011). The diagnosis of dementia due to Alzheimer's disease: recommendations from the National Institute on Aging-Alzheimer's Association workgroups on diagnostic guidelines for Alzheimer's disease. *Alzheimers Dement*, *7*(3), 263–269.

Misra, C., Fan, Y., & Davatzikos, C. (2009). Baseline and longitudinal patterns of brain atrophy in MCI patients, and their use in prediction of short-term conversion to AD: results from ADNI. *NeuroImage, 44*(4), 1415–1422.

Morris, J. C. (1993). The Clinical Dementia Rating (CDR): current version and scoring rules. *Neurology, 43*(11), 2412–2414.

Morris, J. C., Heyman, A., Mohs, R. C., Hughes, J. P., van Belle, G., …, the CERAD investigators (1989). The Consortium to Establish a Registry for Alzheimer's Disease (CERAD): Part 1. Clinical and neuropsychological assessment of Alzheimer's disease. *Neurology*, *39*, 1159–1165.

Mueller, S. G., Weiner, M. W., Thal, L. J., Petersen, R. C., Jack, C. R., …, Beckett, L. (2005). Ways toward an early diagnosis in Alzheimer's disease: the Alzheimer's Disease Neuroimaging Initiative (ADNI). *Alzheimers Dement*, *1*(1), 55–66.

Muthén, B. O. (1997). Latent variable modeling with longitudinal and multilevel data. In A. Raftery (Ed.), *Sociological methodology* (pp. 453–480). Boston: Blackwell.

Muthén, B. O., & Curran, P. J. (1997). General longitudinalmodeling of individual differences in experimental designs: a latent variable framework for analysis and power estimation. *Psychological Methods, 2*, 371–402.

Muthén, L. K., & Muthén, B. O. (1998–2010). *Mplus user's guide: Sixth Edition.* Los Angeles, CA: Muthén & Muthén.

Park, L. Q., Gross, A. L., Pa, J., McLaren, D., Johnson, J. K., Mitchell, M., Manly, J. J., for the Alzheimer's Disease Neuroimaging Initiative (2012). Identification of Invariant Neuropsychological Latent Factors in Alzheimer's Disease from the ADNI Neuropsychological Battery. *Brain Imaging and Behavior*.

Prabhakaran, V., Nair, V. A., Austin, B. P., La, C., Gallagher, T. A., Wu, Y., McLaren, D. G., Xu, G., Turski, P., & Rowley, H. (2012). Current status and future perspectives of magnetic resonance high-field imaging: A summary. *Neuroimaging Clinics of North America*, in press.

Rami, L., Solé-Padullés, C., Fortea, J., Bosch, B., Lladó, A., Antonell, A., Olives, J., Castellví, M., Bartres-Faz, D., Sánchez-Valle, R., & Molinuevo, J. L. (2012). Applying the new research diagnostic criteria: MRI findings and neuropsychological correlations of prodromal AD. *International Journal of Geriatric Psychiatry, 27*, 127–134.

Reitan, R. (1958). Validity of the trail making test as an indicator of organic brain damage. *Perceptual and Motor Skills, 8*, 271–276.

Rey, A. (1964). *L'examen clinique en psychologie*. Paris: Presses Universitaires de France.

Rosen, W. G., Mohs, R. C., & Davis, K. L. (1984). A new rating scale for Alzheimer's disease. *The American Journal of Psychiatry, 141* (11), 1356–1364.

Schott, J. M., Fox, N. C., Frost, C., Scahill, R. I., Janssen, J. C., …, Rossor, M. N. (2003). Assessing the onset of structural change in familial Alzheimer's disease. *Annals of Neurology*, *53*, 181–188.

Seeley, W. W., Crawford, R. K., Zhou, J., Miller, B. L., & Greicius, M. D. (2009). Neurodegenerative diseases target large-scale human brain networks. *Neuron, 62*(1), 42–52.

Shaw, L. M. (2008). PENN biomarker core of the Alzheimer's disease neuroimaging initiative. *Neurosignals, 16*, 19–23.

Shen, L., Qi, Y., Kim, S., Nho, K., Wan, J., …, ADNI. (2010). Sparse bayesian learning for identifying imaging biomarkers in AD prediction. *Medical Image Computing and Computer-Assisted Intervention*, *13*(Pt 3), 611–618.

Smith, C. D., Chebrolu, H., Wekstein, D. R., Schmitt, F. A., Jicha, G. A., …, Markesbery, W. R. (2007). Brain structural alterations before mild cognitive impairment. *Neurology*, *68*, 1268–1273.

Sperling, R. A., Aisen, P. S., Beckett, L. A., Bennett, D. A., Craft, S., …, Phelps, C. H. (2011). Toward defining the preclinical stages of Alzheimer's disease: Recommendations from the National Institute on Aging and the Alzheimer's Association workgroup. *Alzheimers Dement*.

StataCorp. (2011). *Stata statistical software: Release 12*. College Station: StataCorp LP.

Steiger, J. H. (1989). *EZPATH: A supplementary module for SYSTAT and SYGRAPH*. Evanston: Systat.

Talairach, J., & Tournoux, P. (1988). *Co-planar stereotaxic atlas of the human brain*. New York: Thieme.

Thompson, P. M., Mega, M. S., Woods, R. P., Zoumalan, C. I., Lindshield, C. J., …, Toga, A. W. (2001). Cortical change in Alzheimer's disease detected with a diseasespecific population-based brain atlas. *Cerebral Cortex*, *11*, 1–16.

Villemagne, V. L., & Rowe, C. C. (2011). Amyloid imaging. *International Psychogeriatrics, 23*(Suppl 2), S41–S49.

Walhovd, K. B., Fjell, A. M., Dale, A. M., McEvoy, L. K., Brewer, J., Karow, D. S., et al. (2010). Multi-modal imaging predicts memory performance in normal aging and cognitive decline. *Neurobiology of Aging, 31*, 1107–1121.

Wechsler, D. (1987). *Wechsler memory scale-revised*. San Antonio: Psychological Corporation.

Weiner, M. W., Veitch, D. P., Aisen, P. S., Beckett, L. A., Cairns, N. J., …, Trojanowski, J. Q., Alzheimer's Disease Neuroimaging Initiative (2012). The Alzheimer's Disease Neuroimaging Initiative: A review of papers published since its inception. *Alzheimer's & Dementia*, *8*, S1–S68.

Williams, B. W., Mack, W., & Henderson, V. W. (1989). Boston naming test in Alzheimer's disease. *Neuropsychologia, 27*(8), 1073–1079.

Wolk, D. A., & Dickerson, B. C. (2011). Fractionating verbal episodic memory in Alzheimer's disease. *NeuroImage, 54*(2), 1530–1539.